Experimental procedure for the evaluation of tooth stiffness in spline coupling including angular misalignment

Experimental procedure for the evaluation of tooth stiffness in spline coupling including angular misalignment

Francesca Curà, Andrea Mura*

Politecnico di Torino, Department of Mechanical and Aerospace Engineering, C.so Duca degli Abruzzi, 24, 10129 Torino, Italy

A B S T R A C T

Tooth stiffness is a very important parameter in studying both static and dynamic behaviour of spline couplings and gears. Many works concerning tooth stiffness calcula-tion are available in the literature, but experimental results are very rare, above all considering spline couplings. In this work experimental values of spline coupling tooth stiffness have been obtained by means of a special hexapod measuring device. Experi-mental results have been compared with the corresponding theoretical and numerical ones. Also the effect of angular misalignments between hub and shaft has been investigated in the experimental planning.

1. Introduction

Spline couplings and gears are mechanical components used in power transmission systems to transfer torque by means of teeth engaging each other.

Tooth stiffness is a very important parameter influencing their behaviour from both static and dynamic point of view ([1–5]).

As an example, in spline couplings the tooth stiffness may influence both load and pressure distribution along tooth surface [6] and also the corresponding engagement [7].

Many theoretical models are available in the literature for calculating the tooth stiffness of gears and spline couplings [7–14]; the most common model consists of the tooth considered as a cantilever beam [8] subjected to different types of loading, namely: bending, shear, compression, and adding the contribution of the root deformation [9–11]; in particular, the effect of the tooth profile [12], pressure angle [13], and load [14] have been emphasised.

On the contrary, experimental results are very rare; only few works are available in the literature about gear tooth experimental stiffness; as an example Amarnath et al. [15] and Yesilyurta et al. [16] measured the stiffness by means of modal testing procedures in order to assess wear in spur gears; Munro et al. [17] used a standard back-to-back test rig to evaluate the stiffness throughout the full length of the normal path of contact and also into the extended contact region when tooth corner contact occurs.

Concerning spline couplings, literature is completely lacking of experimental works about this topic.

As a matter of fact, in the case of spline couplings, the correct approximation of tooth stiffness is a very important parameter when the pressure distribution has to be exactly calculated, as a little difference in the determination of stiffness may cause a significant variation in the pressure map [18].

* Corresponding author. Tel.: +39 011 090 5907; fax: +39 011 0906 999. *E-mail address:* andrea.mura@polito.it (A. Mura).

Due to the fact that all teeth are engaging in the normal torque transmission, optimisation procedures related to spline couplings are devoted to correctly determine, already in the design phase, the correct pressure distribution on the teeth surface in order to avoid fretting wear, generally being one of the most important failure modes of these components, above all in aerospace applications [19].

Moreover, spline coupling stiffness may influence rotor dynamics and stability in aero engines [3].

The object of the present work is the experimental determination of the tooth stiffness of a spline coupling; to this aim, a special test rig and a dedicated hexapodal displacement measuring device [20,21] have been set up. In particular, the experimental devices (dedicated to the analysis of spline couplings) have an innovative design, being completely new, including the power re-circulating scheme associated with the ability to perform tests in misaligned conditions. Experimental results have been compared to the corresponding obtained by FEM models and analytical approaches. Also the effect of angular misalignment on tooth stiffness has been experimentally investigated. This aspect, is not investigated in the literature, but it is very important because the angular misalignment influence the load distribution on teeth, in terms of pressure distribution, and may cause both undesired fretting wear [22] and additional loads as tilting moments [23].

2. Experimental set up

Tooth stiffness values have been indirectly obtained by measuring the corresponding deformations of a spline coupling subjected to an applied torque.

A dedicated test rig (described in the following section) has been designed in order to apply a constant torque, measured by a torsiometer, and also to allow an angular misalignment between hub and shaft. The deformation of the test article (a spline coupling) has been obtained by means of a dedicated hexapod measuring device (described in the following section) capable of measuring the deformation of all the six degrees of freedom.

Being the aim of this work the exact determination of the tooth stiffness, defined as the ratio between applied torque and measured deformations, the experimental values coming from the hexapod device have to be adjusted for the deformations of the spline coupling core.

2.1. Spline coupling test rig

The test rig used in this work, shown in Fig. 1, has a power re-circulating scheme, allowing a reduction in energy consumption [24].

The test rig is composed (see Fig. 2) of two coaxial shafts (inner and outer) both connected on the right side to a torque generator. The inner shaft is divided into two branches connected by means of the spline coupling test article. On the left end, inner and outer shafts are coupled through a constant-velocity joint (CV-joint). The CV joint decouples the sleeve allowing an equilibrium position to be achieved. When the torque generator applies a torque to the inner shaft, it passes through the test article and comes back, by means of the outer shaft, to the torque generator. This apparatus creates a torque loop putting the spline coupling under load. External and internal shafts (and of course the test article too) can rotate thanks to an electric motor connected to the external shaft by means of a belt.

A lever device allows the creation of an angular misalignment between hub and sleeve of the test article. This deflection is produced by a flexible joint connecting the two parts of the external shaft.

This test rig is equipped with a 5000 Nm torque sensor to measure the torque applied to the test article, a 20 kN load cell to measure the reacting force generated by tilting moments and a linear displacement sensor (LVDT) to measure the angular misalignment between hub and sleeve of the spline coupling.

Fig. 1. Spline coupling test rig.

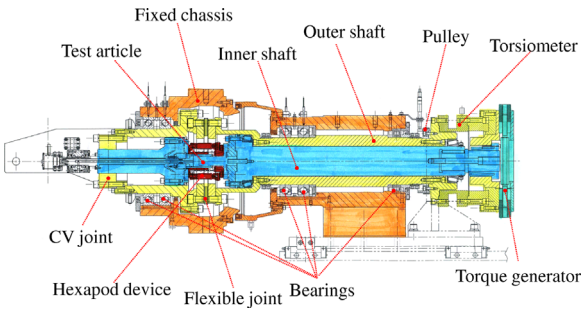

Fig. 2. Schematic of the spline coupling test rig.

2.2. Hexapod displacement measuring device

The hexapod device [20], shown in Fig. 3, is a parallel structure such as a Stewart platform [25] allowing the determination of the relative position between hub and shaft (in terms of the six degrees of freedom: three rotation and three translation), through the measurement of six linear displacements.

This device is composed of a platform and a base connected together by six legs, each containing a linear displacement sensor, as shown in Fig. 4. The legs are connected to the base and the platform by means of spherical joints. The platform and the base are respectively fixed to the shaft and hub flanges (Fig. 5).

When a spline coupling deformation occurs (i.e. the hub and shaft engage with each other), the platform of the measuring device moves with respect to the base, causing an elongation of the six displacement sensors.

In particular, referring to the scheme shown in Fig. 5, when deformation of the spline coupling occurs (being hub and shaft engaged), a relative motion appears between the reference system fixed on the base O_b and the corresponding one fixed on the platform O_p. The position of the local reference system of the platform centred in O_p respect to the local reference system of the base may be given by the homogeneous positioning matrix ${}^{B}\mathbf{A}_{P}$ [20]:

$$ {}^{B}\mathbf{A}_{P} = \begin{bmatrix} E_{11} & E_{12} & E_{13} & p_x \\ E_{21} & E_{22} & E_{23} & p_y \\ E_{31} & E_{32} & E_{33} & p_z \\ 0 & 0 & 0 & 1 \end{bmatrix} \tag{1} $$

The last column of this matrix represents the three translational d.o.f. and the submatrices E_{11}:E_{33} represent the orientation of the two reference systems, that means the relative rotations. Platform rotations may be calculated by the following relations:

$$ \varphi = \tan^{-1}\left(-\frac{E_{12}\ \sin\chi}{E_{11}\ \cos\chi}\right) \tag{2} $$

$$ \chi = \tan^{-1}\left(\frac{E_{13}}{E_{33}\ \cos\psi - E_{23}\ \sin\psi}\right) \tag{3} $$

$$ \psi = \tan^{-1}\left(-\frac{E_{23}}{E_{33}}\right) \tag{4} $$

where φ is the roll angle (around x-axis), χ is the pitch angle (around y-axis) and ψ is the yaw angle (around z-axis) (see Fig. 5). The yaw angle represents the deformation caused by the torque applied on the spline coupling and is used to calculate the tooth stiffness.

Positioning and orientation matrix (1) may be obtained by applying the direct kinematic algorithm to the length of the legs measured by the six LVDT displacement sensors [20]. The direct kinematic equations of the device have been obtained and solved by means of an iterative algorithm written in Matlab environment [20].

The linear displacement sensors incorporated into the legs of the hexapod device are six LVDT Micro-Epsilon DTA-1D-1.5-CA, respectively connected to six signal conditioners Micro-Epsilon MSC 710. Signals are acquired by means of a National Instruments NI USB-6210 board and a dedicated software created in LabView environment. Fig. 6 shows the hexapod displacement measuring device fixed on the test rig.

2.3. Test article and experimental planning

The test article, shown in Fig. 7, consists of an involute spline coupling made of 38NiCrMo4 steel. Hub and shaft are connected to a flange allowing the mounting on the test rig. Table 1 resumes the geometrical characteristics of this spline coupling.

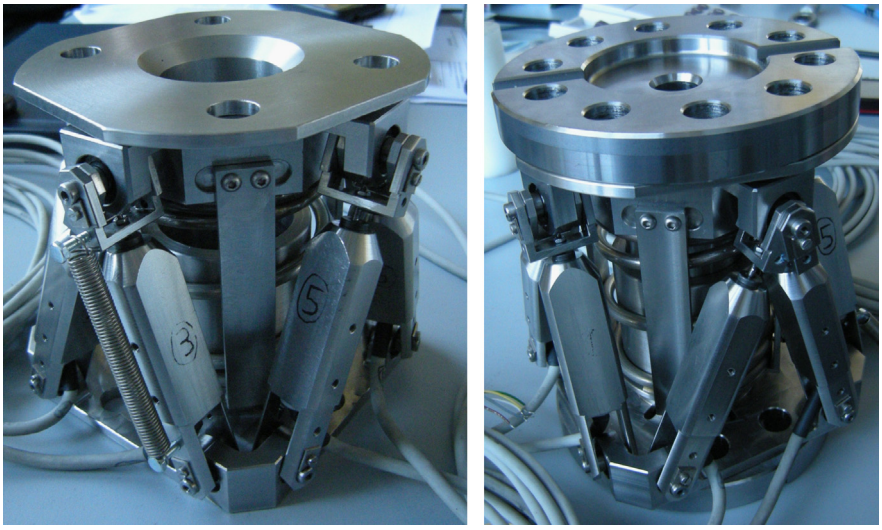

Fig. 3. Hexapod measuring device without (left) and with (right) the spline coupling test article.

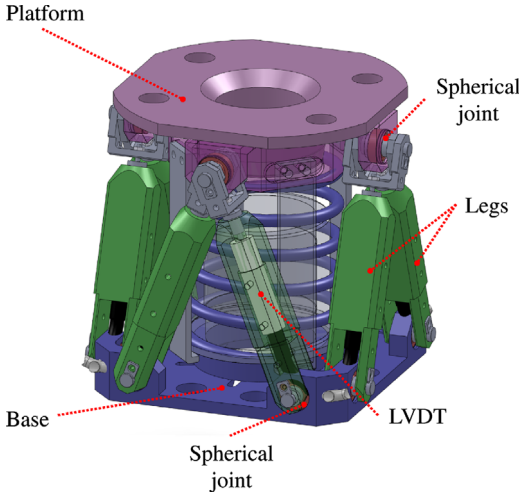

Fig. 4. CAD model of the hexapod measuring device.

Experimental tests have been done applying 15 torque levels from 0 to 700 Nm, with 50 Nm steps. Tests have been conducted with three misalignment levels, 0′, 5′ and 10′, and each test has been repeated three times in order to give the measurements statistical relevance. A total of 135 measurements have been done.

3. Model for the tooth stiffness calculation

The theoretical tooth stiffness has been calculated by the ratio between the applied torque and the angular deformation of the tooth pair obtained by considering the tooth as a cantilever beam [26].

$$K_{Tt} = \frac{T}{\theta_{Tt}} \tag{5}$$

where K_{Tt} is the tooth stiffness, T is the applied torque and θ_{Tt} is the angular deformation.

The angular deformation is determined by the total teeth deformation (considering the deformation of both external shaft teeth and internal hub teeth), obtained as the sum of three components: bending deformation, shear deformation and tooth root deformation (contact deformation has been neglected as in straight involute spline coupling all the involute surface is in contact), as follows:

$$f_{TOT} = f_B + f_S + f_R \tag{6}$$

where f_{TOT}, is the total teeth deformation, f_B is the bending deformation, f_S is shear deformation and f_R is the tooth root deformation.

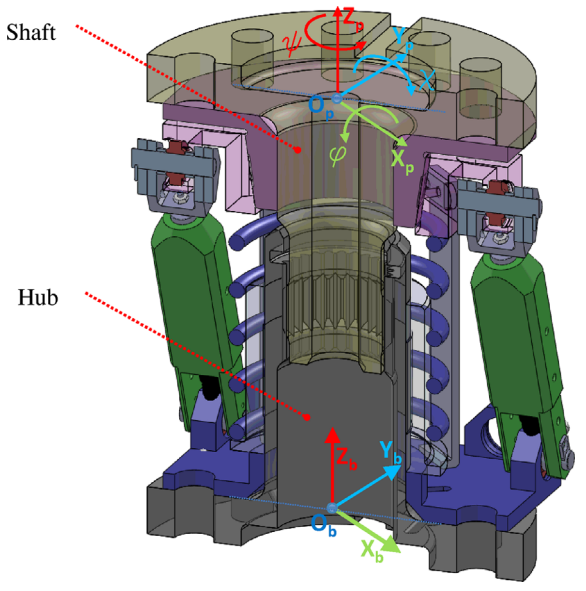

Fig. 5. Hexapod measuring device mounted on the test article.

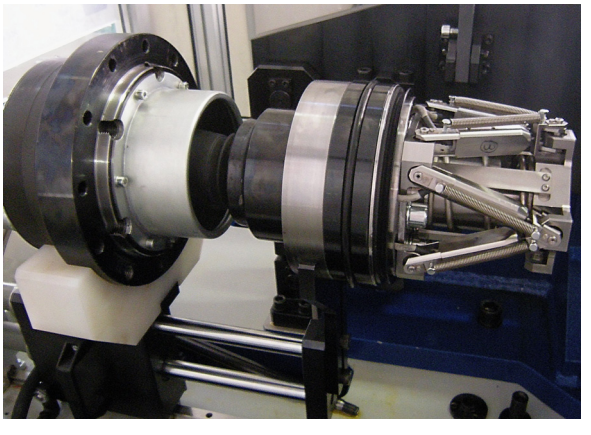

Fig. 6. Hexapod measuring device mounted on the test rig sleeve.

Fig. 7. Test article.

Table 1
Parameters of the spline coupling.

Pitch diameter [mm]	33.02
Modulus [mm]	1.27
Number of teeth	26
Pressure angle [deg.]	30
Shaft external diameter [mm]	34.77
Sleeve internal diameter [mm]	31.32

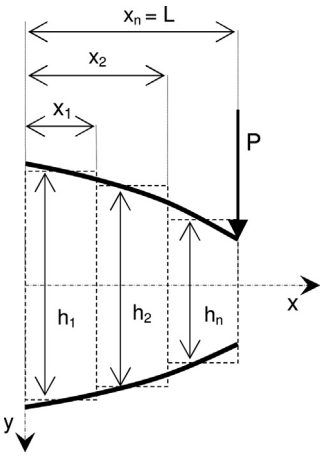

Fig. 8. Model of the tooth splitted into slices.

In spline couplings the load is transferred, in nominal conditions, by the contact of the two sides of the engaging teeth so the load is distributed along the contact surface. To simplify the problem, the load P is considered applied at a single point corresponding with the pitch diameter [26].

To calculate bending and shear deformations, the tooth has been split into n slices, as shown in Fig. 8, and the deformation has been obtained as the sum of the deformations of each slice. Distances $x(i)$ ($x_1, x_2,\ldots x_n$) refer to the coordinate difference between tooth root and ith slice. Bending deformation δ_F has been obtained by the integral calculation of the elastic curve [27].

$$\delta_F = \int_0^{x1} \frac{M(x)}{EI_1} A_1 x\, dx + B_1 + \cdots + \int_{xi}^{xi+1} \frac{M(x)}{EI_i} A_i x\, dx + B_i + \cdots + \int_{xn-1}^{xn} \frac{M(x)}{EI_n} A_n x\, dx + A_n \tag{7}$$

where $M(x)$ is the bending moment acting at the ith slice, E is Young's modulus of the material, I is the second moment of area of the ith slice, A_i and B_i are the ith integration constants.

Integration constants A_1 and B_1 have been obtained by considering as boundary conditions nil rotation and deformation at the clamped side of the beam is (x=0) (Eqs. (8) and (9)). Other constants have been obtained by imposing the coherence of both rotations and deformations at the joint of each slice (Eqs. (10) and (11)).

$$A_1 = \frac{P(L)^2}{2EI_1} \tag{8}$$

$$B_1 = \frac{P(L)^3}{6EI_1} \tag{9}$$

$$A_i = \frac{P(L-x_{i-1})^2}{2EI_i} - \frac{P(L-x_{i-1})^2}{2EI_{i-1}} + A_{i-1} \tag{10}$$

$$B_i = \frac{P(L-x_{i-1})^3}{6EI_i} + A_{i-1}x_{i-1} + B_{i-1} - \frac{P(L-x_{i-1})^3}{6EI_{i-1}} + A_i x_{i-1} \tag{11}$$

where P is the load applied on the tooth (x=L) and L is the x_n distance along the teeth involute (see Fig. 8).

Shear deformation δ_T has been obtained by the integral calculation of the corresponding displacement [27] (Eq. (12)):

$$\delta_T = \int_0^{x1} \chi \frac{P}{GC_1} x_1 + C_1 + \cdots + \int_{xi}^{xi+1} \chi \frac{P}{GC_i} x_i + C_i + \cdots + \int_{xn-1}^{xn} \chi \frac{P}{GC_n} x_n + C_n \tag{12}$$

where χ is the shear deformation factor, G is the shear elastic modulus and C_i is the ith integration constant.

First integration constant C_1 has been obtained by imposing nil deformation at the clamped side of the beam ($x=0$).

$$C_1 = 0 \tag{13}$$

Other constants have been obtained by imposing the correspondence of deformations at the joint of each slice as follows:

$$C_i = \chi \frac{P}{GC_{i-1}} x_{i-1} - \chi \frac{P}{GC_i} x_{i-1} + C_{i-1} \tag{14}$$

The tooth root deformation δ_R has been calculated by the O'Donnell formulation [12]:

$$\delta_R = P \frac{\cos^2 \alpha}{WE} \left[\frac{16.67}{\pi} \left(\frac{L}{h} \right)^2 + 2(1-\nu) \left(\frac{L}{h} \right) + 1.534 \left(1 + \frac{\tan^2 \alpha}{2.4(1+\nu)} \right) \right] \tag{15}$$

where α is the load inclination angle, h is the tooth thickness at L and W is the tooth width.

4. FEM model

A 3D FEM model of the spline coupling, created by means of the software Solid Works Simulation, has been done to also obtain numerical results for the tooth stiffness. The FEM model has been realised by considering the shaft and hub separately (Fig. 9). The mesh consists of 519,863 nodes and 360,427 second-order tetrahedral elements.

Shaft and hub have been bounded respectively on internal and external diameter. The load has been applied on each tooth by a distributed force along the tooth width, on the pitch diameter; 14 load cases have been considered corresponding to torque levels from 50 to 700 Nm (with 50 Nm load step).

It may be considered that the deformation measured by means of the hexapod device represents the relative rotation of the two flanges connected to the spline coupling: this means that the measured deformation is due not only to the tooth deformation, but also that of the shaft. To obtain the contribution due only to the teeth, the shaft deformation calculated by means of the classical theory of elasticity formula [27] has been subtracted from the measured deformation, and verified by means of another FEM model, according to the scheme represented in Fig. 10. In particular, the spline coupling is divided into three zones one representing the female shaft, one representing the male shaft and the other representing the teeth.

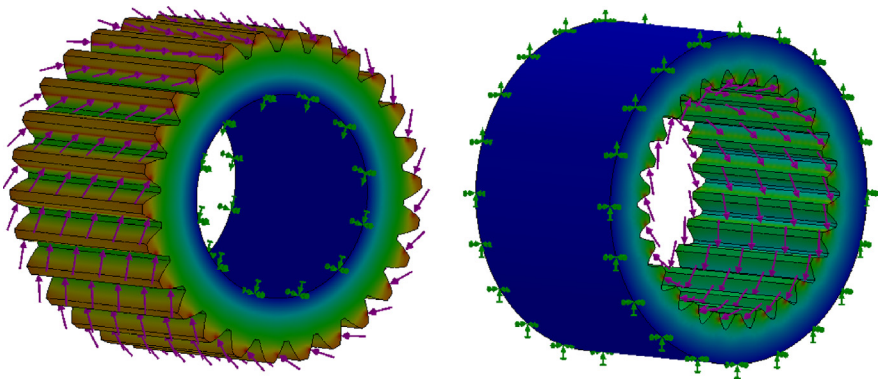

Fig. 9. Spline coupling FEM model.

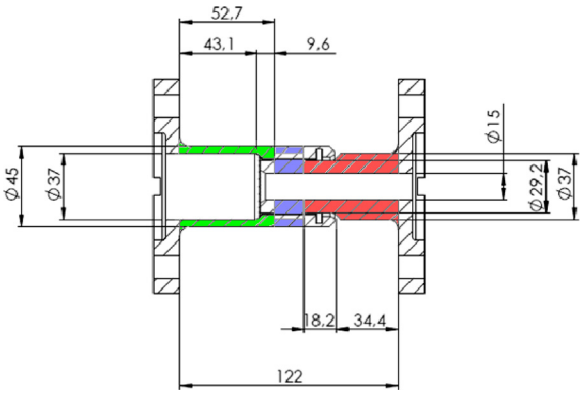

Fig. 10. Scheme of the spline coupling.

The FEM model has been created by dividing the spline coupling according to the scheme represented in Fig. 10, with the flange bounded and the torque applied on the shaft free end.

5. Results and discussion

Results have been reported in terms of deformations varying both torque level and angular misalignments.

Fig. 11 shows the measured deformations of the spline coupling (singular and average values) without misalignment.

Fig. 12 shows the average tooth deformations obtained from experimental results (removing the shaft deformation, as described in Section 4), compared with FEM and theoretical ones.

It is possible to observe that the stiffness values obtained by the three methods match very well; in particular, the maximum difference between experimental and FEM results is 7.6% and the maximum difference between experimental and theoretical results is 8.5%.

It is possible to highlight that the results obtained by means of FEM models are generally more stiff than the corresponding experimental ones; this phenomenon is more evident for higher torque values.

Otherwise, theoretical results involve a little lower deflection with respect to the corresponding FEM ones; this effect is probably due to a different approach in simulating the boundary conditions (one tooth is considered in the theoretical model, the whole component in the FEM one).

Anyway, as observed before, the difference between the three methods is very little and it is possible to point out that all methods used in this work are suitable to calculate tooth deformation and the corresponding stiffness.

On the basis of the very good agreement obtained between all results (experimental, FEM and theoretical) for the aligned case, a corresponding reliability may be assigned to the experimental investigation about the effect of the misalignment angle.

Figs. 13 and 14 show the experimental deformations obtained respectively by imposing 5′ and 10′ angular misalignments.

In order to evaluate the effect of angular misalignment on the coupling stiffness, average experimental deformations, referring to 0′, 5 ′ and 10′ misalignment values respectively, have been compared in Fig. 15.

It is possible to observe that the tooth deformation increases by increasing the angular misalignment angle.

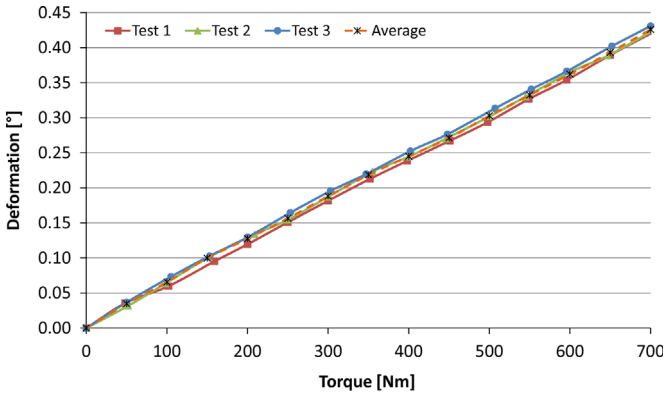

Fig. 11. Experimental deformation for 0′ of angular misalignment.

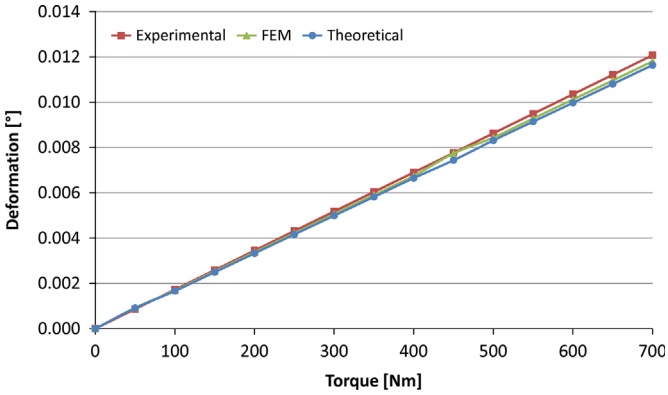

Fig. 12. Comparison between experimental, FEM and theoretical results.

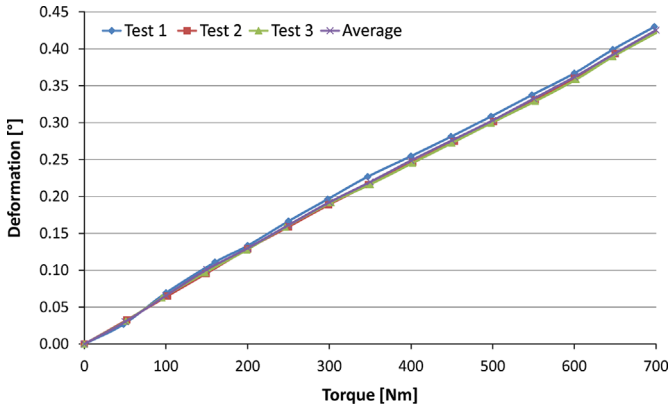

Fig. 13. Experimental deformation for 5′ of angular misalignment.

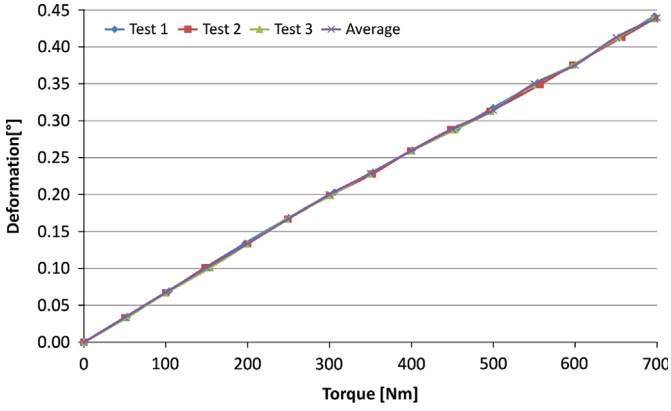

Fig. 14. Experimental deformation for 10′ of angular misalignment.

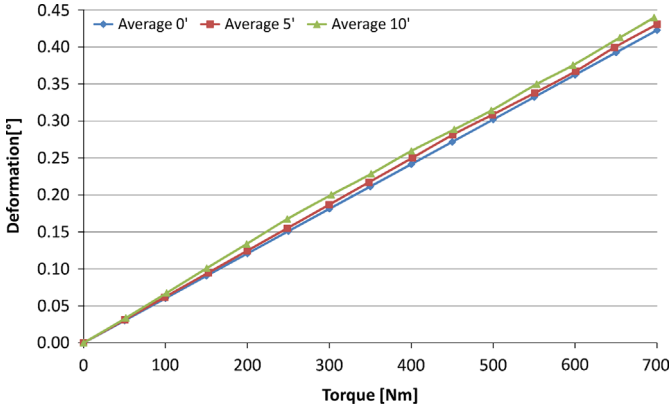

Fig. 15. Effect of angular misalignment on spline coupling deformation.

Considering the average stiffness value obtained by the ratio between the applied torque and the relative deformation, it is possible to point out (Fig. 16) that by increasing the angular misalignment, the tooth stiffness decreases.

This is justified because of in misaligned spline couplings only a part of the teeth face width is in contact: in this way the deformation due to the applied torque is higher than in the aligned conditions [23] and so the resultant tooth stiffness decreases.

The above quoted phenomenon is related to a variation of the pressure distribution on the tooth contact surface, that may change its behaviour when the spline coupling is misaligned [23] with respect to the case of an aligned spline coupling [1].

Generally speaking a tooth stiffness variation may affect not only the static behaviour of a component, but also the corresponding dynamic behaviour [2]; a correct information about both stiffness value and parameters influencing the corresponding stiffness variation allows a good prediction of the component behaviour already in the design phase.

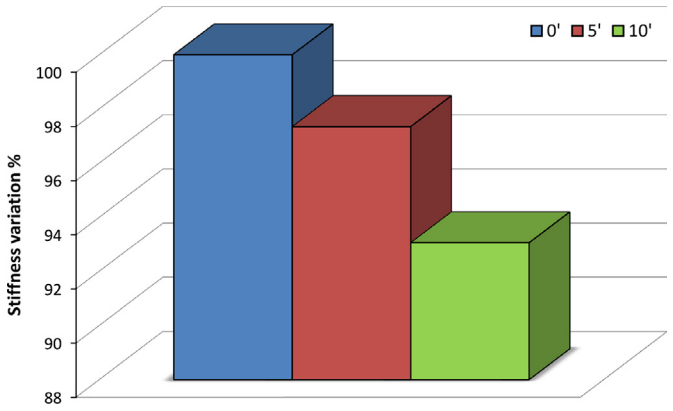

Fig. 16. Effect of angular misalignment tooth stiffness.

6. Conclusions

This paper deals with an investigation about tooth stiffness in spline couplings carried on by means of experimental, theoretical and numerical techniques.

In particular, experimental values of the tooth stiffness have been obtained by means of a dedicated test rig and an apposite deformation measuring device. The experimental equipments showed a very good behaviour during the tests, allowing to apply the right load to the specimen and to properly measure the spline coupling deformation also in misaligned conditions.

Theoretical values have been determined by applying the classical formulas for beams to a discretised model of the tooth.

Experimental values have been compared with FEM and theoretical results, showing a very good agreement. This means that the theoretical model used to calculate the tooth stiffness (taking into account bending, shear and tooth root deflection) is appropriate to a good estimation of spline coupling tooth stiffness.

The effect of angular misalignments on tooth stiffness has also been taken into account; this is a very important point, because literature is lacking about investigation on this topic. Results show that by increasing the angular misalignment, the stiffness decreases with a non-linear behaviour; this result agrees well with the physical behaviour of the mechanical system under study.

References

[1] A. Barrot, M. Paredes, M. Sartor, Extended equations of load distribution in the axial direction in a spline coupling, Eng. Failure Anal. 16 (1) (2009) 200–211.
[2] L. Shuguo, M. Yanhong, Z. Dayi, H. Jie, Studies on dynamic characteristics of the joint in the aero-engine rotor system, Mech. Syst. Signal Process. 29 (2012) 120–136.
[3] R.G. Parker, S.M. Vijayakar, T. Imajo, Non-linear dynamic response of a spur gear pair: modelling and experimental comparisons, J. Sound Vib. 237 (3) (2000) 435–455.
[4] K.J. Huang, T.S. Liu, Dynamic analysis of a spur gear by the dynamic stiffness method, J. Sound Vib. 234 (2) (2000) 311–329.
[5] C.J. Li, H. Lee, Gear fatigue crack prognosis using embedded model, gear dynamic model and fracture mechanics, Mech. Syst. Signal Process. 19 (2005) 836–846.
[6] V. Cuffaro, F. Curà, A. Mura, Analysis of the pressure distribution in spline couplings, Proc. Inst. Mech. Eng. Part C: J. Mech. Eng. Sci. 226 (12) (2012) 2852–2859, http://dx.doi.org/10.1177/0954406212440670.
[7] J. Silvers, C.D. Sorensen, K.W. Chase, A new statistical model for predicting tooth engagement and load sharing in involute splines, AGMA Technical Resources, 2010, ISBN:978-1-55589-982-0.
[8] R.W. Cornell, Compliance and stress sensitivity of spur gear teeth, ASME J. Mech. Des. 103 (1981) 447–459.
[9] F. Chaari, T. Fakhfakh, M. Haddar, Analytical modelling of spur geartooth crack and influence on gearmesh stiffness, Eur. J. Mech.—A/Solids 28 (3) (2009) 461–468.
[10] W.J. O'Donnell, The additional deflection of a cantilever due to the elasticity of the support, J. Appl. Mech. 27 (1960) 461–464.
[11] F. Vogt, About Root Foundation Deformation (Über die Berechnung der Fundamentdeformation), Avhandling ved Det Norske Videnskaps Akademi, I. mathematisk-naturvidenskabelig Klasse no. 2, Oslo Dybvad, 1925.
[12] Y. Terauchi, K. Nagamura, Study on deflection of spur gear teeth (2nd report, Calculation of tooth deflection for spur gears with various tooth profiles), JSME 24 (188) (1981) 447–452.
[13] S. Oda, T. Koide, T. Ikeda, K. Umezawa, Effects of pressure angle on tooth deflection and root stress, Bull. JSME 29 (255) (1986) 3141–3148.
[14] C. Weber, The Deformation of Loaded Gears and the Effect on their Load Carrying Capacity, Sponsored Research (Germany), British Department of Scientific and Industrial Research, Report no. 3, 1949.
[15] M. Amarnath, C. Sujatha, S. Swarnamani, Experimental studies on the effects of reduction in gear tooth stiffness and lubricant film thickness in a spur geared system, Tribol. Int. 42 (2009) 340–352.
[16] I. Yesilyurta, F. Gub, A.D. Ball, Gear tooth stiffness reduction measurement using modal analysis and its use in wear fault severity assessment of spur gears, NDT & E Int. 36 (5) (2003) 357–372.
[17] R.G. Munro, D. Palmer, L. Morrish, An experimental method to measure gear tooth stiffness throughout and beyond the path of contact, Proc. Inst. Mech. Eng. Part C J. Mech. Eng. Sci. 215 (7) (2001) 793–803.
[18] A. Barrot, M. Paredes, M. Sartor, Determining both radial pressure distribution and torsional stiffness of involute spline couplings, Proc. Inst. Mech. Eng. Part C: J. Mech. Eng. Sci. 220 (12) (2006) 1727–1738.

[19] J. Ding, W.S. Sum, R. Sabesan, S.B. Leen, I.R. McColl, E.J. Williams, Fretting fatigue predictions in a complex coupling, Int. J. Fatigue 29 (2007) 1229–1244.[20] A. Mura, Six d.o.f. displacement measuring device based on a modified Stewart platform, Mechatronics 21 (2011) 1309–1316.
[21] Mura A., Sensitivity analysis of a six degrees of freedom displacement measuring device, Proc. Inst. Mech. Eng. Part C: J. Mech. Eng. Sci. (2013) http://dx.doi.org/10.1177/0954406213482071.
[22] S. Medina, A.V. Olver, An analysis of misaligned spline couplings, Proc. Inst. Mech. Eng. Part J: J. Eng. Tribol. 216 (2002) 269–279.
[23] A.H. Elkholy, M.A. Alfares, Misalignment loads in splined gear coupling, Int. J. Comput. Appl. Technol. 15 (1–3) (2002) 128–137.
[24] F. Curà, A. Mura, V. Cuffaro, M. Facchini, Banco prova per alberi scanalati (A Test Rig for Spline Couplings), AIAS—Associazione Italiana per l'Analisi delle Sollecitazioni 41° Convegno Nazionale, 5–8 settembre 2012, Università degli Studi di Padova (in Italian).
[25] D. Stewart, A platform with six degrees of freedom, Proc. Inst. Mech. Eng. London 180 (1965) 371–386.
[26] F. Curà, A. Mura, M. Gravina, Load distribution in spline coupling teeth with parallel offset misalignment, Proc. Inst. Mech. Eng. Part C: J. Mech. Eng. Sci. (2012) http://dx.doi.org/10.1177/0954406212471916.
[27] S.P. Timoshenko, J.N. Goodier, Theory of Elasticity, McGraw-Hill, New York, 1970.